Preparation and Morphological Characterization of Two- and Three-Component Natural Rubber-Based Latex Particles

MICHAEL SCHNEIDER, THA PITH, and MORAND LAMBLA*

Ecole d'Application des Hauts Polymères, Institut Charles Sadron (CRM-EAHP), 4, rue Boussingault, Strasbourg, France

SYNOPSIS

Different emulsion polymerization processes allowed variation in the microstructure of composite natural rubber (NR)-based latex particles. A prevulcanized and a not-crosslinked natural rubber latex were coated with a shell of crosslinked poly(methyl methacrylate) (PMMA) or polystyrene (PS). The bipolar redox initiating system *tert*-butyl hydroperoxide/tetraethylene pentamine promoted a core–shell arrangement. Furthermore, PS subinclusions were introduced into the NR core. The initiators used for the subinclusion synthesis were azobisisobutyronitrile at high temperature and a redox initiation system consisting of *tert*-butyl hydroperoxide/dimethylaniline at low temperature. The morphology of the resulting latex interpenetrating networks (IPN) was characterized by transmission electron microscopy (TEM) and scanning electron microscopy (SEM). Different staining methods allowed us to increase the contrast between the NR phase and the secondary polymers in the composite latex particles. A semicontinuous feeding process decreased the PS subinclusions size by a factor of 6 in comparison with a batch reaction. Depending on the NR/styrene swelling ratio, the crosslinking degree, and the polymerization temperature used, distinct differences of the phase arrangement of polymers in the latex particles were revealed.

INTRODUCTION

Control of latex particle morphology by seeded emulsion polymerization is well known in industry. Many latex applications such as adhesives, coatings, impact modification, and toughening of polymers depend on it.[1-3] Latex particles with different morphological structures can be prepared from seeded emulsion polymerization techniques.[4,5] These particles typically comprise an inner soft polymer sphere, i.e., the "core," and an outer hard polymer "shell." Although particles may be prepared in two consecutive stages, a core–shell structure does not necessarily result. In the literature, many examples of other phase arrangements like, e.g., "raspberry-like," "acornlike," "sandwichlike," "poow," and inverted structures are found.[6-9] Figure 1 schematically represents these structures.

Many different parameters like, e.g., the monomer addition sequence, the hydrophilicity of the monomers and polymers, the used initiating systems, and the viscosity within the monomer swollen seed latex particles have to be taken into account. The last factor is primarily determined by the reaction temperature, the degree of crosslinking of the polymer chains, the monomer concentration in the seed latex particle during the reaction, and the molecular weight of the polymers. Furthermore, thermodynamic and kinetic aspects have to be considered. A morphology with the lowest free energy G is only achieved when the mobility of polymer chains is not too much reduced by a very high viscosity within the monomer swollen latex particle.

In this article, the preparation of composite natural rubber (NR)-based latex particles is described. It is an extension of earlier studies of the modifi-

* To whom correspondence should be addressed.

Journal of Applied Polymer Science, Vol. 62, 273–290 (1996)
 CCC 0021-8995/96/020273-18

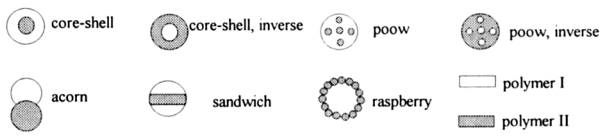

Figure 1 Possible morphologies of composite latex particles.

cation of NR while still in latex form.[10–14] Although modified NR latexes have been exploited industrially for 40 years, many of the fundamental processes involved in the formation of specific morphologies remain poorly understood. A redox-initiating system consisting of *tert*-butyl hydroperoxide (*tert*-BuHP) and tetraethylene pentamine (TEPA) proved to be very effective for emulsion polymerization in an NR latex: It is not sensitive to oxygen and works well with ammonia present. A surfactant (usually a fatty acid soap) protects the latex against coagulation. Virtually all commercial processes for grafting monomers onto NR are based on this type of redox polymerization.[15] Composite NR latexes of this type are known as *Heveaplus*.[16] Another method of initiation consists of a pretreatment of the NR latex with a hydroperoxide and an activator followed by the addition of methyl methacrylate and a stabilizer.[17] It is also possible to employ a fully oil soluble redox system consisting typically of benzoyl peroxide and dimethylaniline (DMA).[18] The grafting efficiency is comparable to the *tert*-BuHP/TEPA-based initiation system. An inactivated polymerization with hydroperoxides, azobisisobutyronitrile (AIBN), or persulfates can also be used, but proves to be less effective than are the activated systems. Last but not least, γ-radiation-induced copolymerization in a monomer-swollen NR seed latex is possible.[19,20]

In 1958, Allen et al.[21] determined in detail the grafting mechanism by using tracer methods. The reaction mechanism is schematically represented by the following equations:

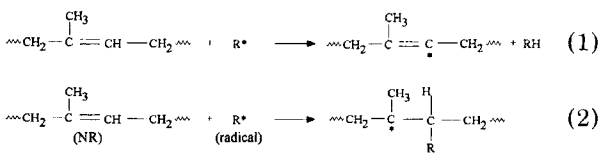

The addition reaction (2) plays a minor role in relation to the transfer reaction (1). The equations explain also the mechanism in solution or in solid rubber, swollen with a monomer containing the initiator.

The present investigation is concerned with the emulsion polymerization of styrene (St) and methyl methacrylate (MMA) in a prevulcanized and a not-crosslinked NR latex to obtain composite NR latex particles. Their morphology was investigated as a function of the addition method and the used initiation systems. One of the most important aspects of the graft copolymerization in an NR latex is the site of the polymerization.[22,23] Investigations by Andrews and Turner[24] and Allen et al.[21,25] suggest that the nature of the different initiating systems determines primarily the morphological structure of composite NR-based latex particles. We chose a bipolar redox initiator couple consisting of *tert*-BuHP and TEPA to promote a core–shell morphology. Furthermore, crosslinked polystyrene (PS) subinclusions were introduced into the NR core using AIBN initiation or the hydrophobic redox initiation system *tert*-BuHP/DMA (*tert*-BuHP/DMA). The emulsion polymerization procedures used for the preparation of these composite latex particles determine whether the NR chains will be grafted or not. This difference is due to the grafting mechanism which is based on a direct initiator attack on the NR molecule. The redox initiation system *tert*-BuHP/DMA is known to graft NR chains. On the other hand, AIBN initiation does not graft NR chains because of the inferior resonance stabilization of 2-cyano-2-propyl radicals. The prepared composite NR-based particles can be classified as interpenetrating (IPN) or semi-interpenetrating latex networks (semi-IPN) combining a rubber and a thermoplastic polymer. An IPN is defined as a combination of two polymer networks, which were prepared in such a manner that at least one has been synthesized and/or crosslinked in the presence of the other.[26]

One possible application of the prepared composite NR-based latex particles is their use as impact modifiers for poly(methyl methacrylate) (PMMA),[27] PS,[28] poly(styrene-*co*-acrylonitrile),[29] and polycarbonate/PS or poly(styrene-*co*-acrylonitrile) ternary blends.[29] The composite NR-based latex particles possess a polar PMMA shell around the rubber core in order to compatibilize the rubbery particles with different polymer matrices. A hard shell which is encapsulating the soft rubber core is needed for the continuous blending preparation process in a twin-screw extruder. NR has an overall balance of properties which is unmatched by synthetic polymers.

EXPERIMENTAL

Materials

A centrifuged prevulcanized NR latex "*Revultex MR*" and a not-crosslinked NR latex "*Revertex AR*" of Revertex Co., with a solids content of 60% were used as seed latexes in an emulsion polymerization. Photon correlation spectroscopy performed on a Malvern Autosizer II gave 500 nm as the *z*-average mean value for the particle size of prevulcanized and not-crosslinked NR latexes.

Figure 2 shows that the particle-size distribution curves of both seed latexes are very similar. The very polydisperse distribution curves are situated between 0.2 and 2 μm.

Deionized water was used in all experiments. Styrene (Fluka AG) was purified by passing through an aluminum oxide column and MMA (Atochem) was distilled. Ethylene glycol dimethacrylate (EGDMA, Merck), *tert*-BuHP (70% aqueous solution, Merck), TEPA (Fluka AG), DMA (Fluka AG), AIBN (Merck), and the surfactant *AD-33* (37% aqueous solution of an ammonium nonylphenylether sulfate, Seppic) were used as received. The antibacterial agent "Preventol DG" of Bayer was added to protect the NR latexes against microorganisms.

Synthesis of PS Subinclusions Within NR particles

Latex semi-IPNs consisting of not-crosslinked NR and crosslinked PS were synthesized in a stirred stainless-steel batch reactor (5 L). Preliminary trials were performed in a 1 L glass reactor to determine the optimal polymerization conditions. The reactors were purged with nitrogen. Crosslinked PS subinclusions, 20, 40, or 60 wt %, were introduced into the NR-based latex particles.

A hydrophobic redox initiation system of *tert*-BuHP and DMA (ratio 1/1, 0.50 wt % based on NR) served for the preparation of different latex semi-IPNs. First, the noncrosslinked NR rubber seed latex was diluted with distilled water so that the final latex solids content was 40%, and 1.5 wt % based on the final solids content of the surfactant AD-33 was added. Then, a solution of St containing the activator DMA and 0.25 wt % of the crosslinking agent EGDMA was stirred into the seed latex for 10 min. After a period of 30 min, the initiator *tert*-BuHP was added and the temperature was increased to 50°C for 12 h.

Furthermore, 0.40 wt % AIBN based on NR was used as the initiator. First, the non-crosslinked NR rubber seed latex was diluted with distilled water to obtain a final composite NR latex with a solids content of 50%. Second, 1.0 wt % of the surfactant AD-33 based on the monomer was added to the diluted NR latex. Then, a mixture of St containing 0.25 wt % DMAEG and the initiator was pumped into the agitated NR latex for 10 min. The reactor was stirred for 3 h at room temperature before the temperature was increased to 70°C to start the polymerization. After a reaction time of 5 h, the temperature was increased to 85°C for 1.5 h to finish the reaction. The degree of conversion was determined gravimetrically.

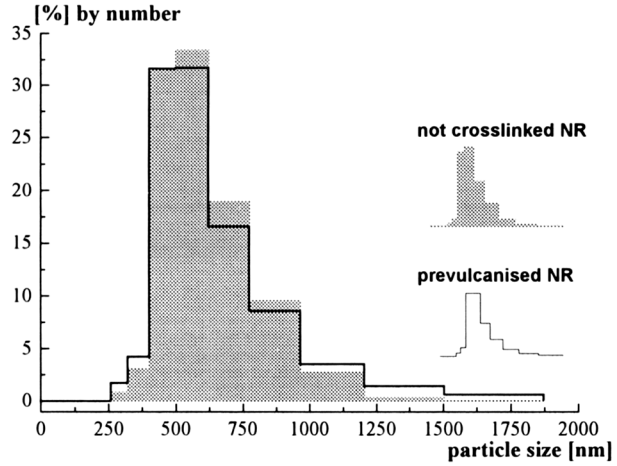

Figure 2 Size-distribution curve of a prevulcanized and a not-crosslinked NR-based latex.

Synthesis of NR-based Core–Shell Particles

A not-crosslinked or prevulcanized NR latex was charged into a stirred stainless-steel reactor (5 L). After the system was purged by nitrogen, St, or MMA, emulsions were fed continuously into the main reactor which was thermostated at 50°C. Water was added to the seed latex and the monomer preemulsion to maintain the latex solids content at 50%. The monomers always contained 0.25 wt % of EGDMA as the crosslinking agent. The surfactant AD-33, 1.0 wt %, based on the monomers was added to the preemulsion. The bipolar redox initiating system *tert*-BuHP/TEPA was employed in the ratio 1/1. In the case of the MMA polymerization, 0.20 wt % of the initiator system based on NR was used. The needed quantity of the initiator had to be increased to 0.30 wt % for the St polymerization. Prevulcanized NR required 1.0 wt % of the initiator system based on NR. The activator TEPA was added into the main reactor together with the NR seed latex, whereas the initiator *tert*-BuHP was fed to-

gether with the preemulsion at a feeding rate of 5 mL/min (MMA) or 2.5 mL/min (St). After the addition of the monomer preemulsion, the temperature was maintained for 2 h at 50°C to finish the reaction. The degree of conversion was determined gravimetrically. Not-crosslinked NR seed latexes containing PS subinclusions were coated in the same way. Table I summarizes a typical recipe for a composite NR latex containing 30 wt % crosslinked PS subinclusions within the NR core and 25 wt % crosslinked PMMA in the shell.

Electron Microscopy

A Cambridge Instruments Stereoscan 120 scanning electron microscope was used for the examination of latex samples which were prepared in the following way: A diluted drop of latex was put onto an aluminum support and subsequently put into liquid nitrogen. Then, a gold layer was deposited on the still frozen support with a Cambridge Instruments sputter coater.

A Phillips EM 300 transmission electron microscope (TEM) was used to observe ultramicrotome cuts of latex particles which had been incorporated into a PS matrix. First, a smooth surface of the PS blend was exposed to osmium tetroxide vapors for 48 h to stain the NR phase.[30-32] The staining not only enhanced the contrast for the microscopic viewing of the blends but also hardened the rubber phase. In this way, ultramicrotome cuts could be prepared without altering the particle morphology of the no longer soft rubber particles. Furthermore, latex particles, which were deposed onto a collodion film, were observed. The PMMA shell was stained with a solution of 2% phosphotungstic acid (PTA) for 2 h.

Differential Scanning Calorimetry

A 10–20 mg sample of a dried latex film was placed into an aluminum pan and measured between −80 and 140°C in a Perkin-Elmer DSC4 thermal analyzer. The heating and cooling rate was 10°C/min.

Dynamic Mechanical Measurements

The measurements were performed on a Rheometrics RSA II instrument which was operated at a frequency of 10 rad/s between −100 and 0°C. Each specimen was stepwise heated from −100°C in intervals of 2.5°C and conditioned at the desired temperature for 2 min before each measurement. Specimens (radius 4 mm, 2 mm thickness) were cut out of cast films which were left at 23°C and 50% relative humidity for 2 weeks.

Thermogravimetric Analysis

A Mettler TA3000 thermogravimetric analyzing system was used to follow the weight loss of a 20 mg NR latex sample between 35 and 800°C while the system was purged with ordinary air. The heating rate was 10°C/min.

RESULTS AND DISCUSSION

The influence of the emulsion polymerization processes, and especially the used initiation systems, was the primary concern of this study. NR-based core–shell particles have never been purposely prepared. Previous research was concentrated on the grafting process and the obtained morphological structure was of secondary interest. A centrifuged prevulcanized NR latex and a not-crosslinked NR

Table I Recipe for a Composite NR Latex Containing 30 Wt % Crosslinked PS Subinclusions Within the NR Core and 25 Wt % Crosslinked PMMA in the Shell

First Stage		Second Stage	
Main reactor		Main reactor	
Not-crosslinked NR (60%)	1875 g	Seed latex (first stage)	3760 g
St	748 g	Activator (TEPA)	2.2 g
EGDMA	2 g	Feeding tank	
AD-33 (37% in water)	20 g	MMA	623 g
AIBN	4.5 g	EGDMA	1.6 g
Water	1112 g	AD-33 (37% in water)	17 g
		tert-BuHP (70% in water)	3.2 g
		Water	613 g

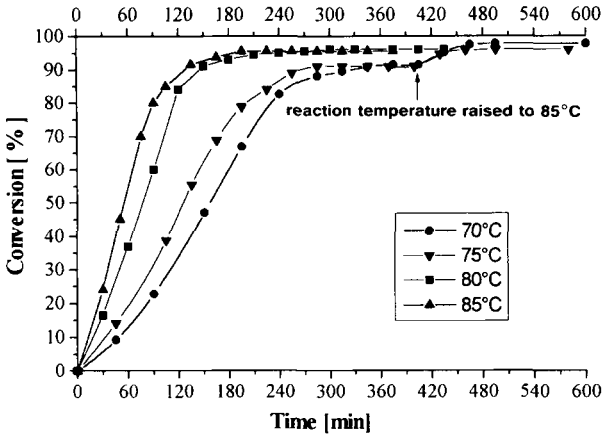

Figure 3 Conversion–time plots for the polymerization of St in the presence of a NR seed latex using 0.40 wt % AIBN based on NR at 70, 75, 80, and 85°C. St/NR weight ratio: 40/60.

latex with a *z*-average mean particle size of 500 nm were used as seed latexes in a sequential emulsion polymerization. A semicontinuous reaction process which favors core–shell arrangements in latex particles was applied. PS subinclusions were synthesized in a batch reactor. Besides, a very effective commercial surfactant was used. The resulting copolymers possess novel characteristics in relation to the already existing range of composite NR particles. PMMA- and PS-grafted composite NR latex particles were synthesized. Since NR latexes contain many nonrubber substances such as proteins which act as polymerization inhibitors,[33] a relative large quantity of initiator calculated on the amount of NR was necessary in all cases. A characterization of proteins and lipids in NR latexes can be found in the literature.[34]

Batch Emulsion Polymerization: Subinclusion Synthesis

AIBN initiation was used for the PS subinclusion synthesis because AIBN is not soluble in the water phase. The polymerization takes place in the organic phase and very little occurs in the aqueous phase. Furthermore, AIBN initiation provides more hydrophobic PS chains compared to the sulfate-ended PS macromolecules resulting from persulfate initiation. Since the seed latex particles are large, the polymerization in the interior of the particles resembles a bulk polymerization. Very accurate measurements on the kinetics of the polymerization of vinyl monomers in NR latexes can be found in the literature.[33,35] The concern of this research project was only to establish the exact polymerization conditions for maximal conversion. Relative large amounts of AIBN have to be used because of the retarding effect of nonrubber substances in NR latexes. The two main factors to be considered are the amount of the used initiator and the reaction temperature. The soap concentration (1.0 wt % AD-33 based on St), NR seed latex/monomer weight ratio (60/40), crosslinking degree (0.25% EGDMA based on St), and solids content of the latex (50%) were kept constant. The greater hydrophobicity of St relative to the NR seed latex particles should assure that the monomer uniformly swells the rubber particles at room temperature and the subsequent polymerization should take place in the interior of the monomer swollen NR particles. The time t_{eq} required to achieve equilibrium swelling of a latex particle by a small molecule has been estimated as 20 times the sorption half-time[36]:

$$t_{eq} = (20)\ 7.66 \times 10^{-3}\ D^2/D_s$$

where D is the particle diameter, and D_s, the diffusion coefficient of a small molecule in the latex particle. For an NR particle with a *z*-average mean diameter of 500 nm, equilibrium swelling by St occurs in 10 min if D_s exceeds 6.4×10^{-13} cm^2/s. Values of D_s for organic liquids in polymers above their T_g are on the order of 10^{-8} and 10^{-10} cm^2/s.[37] The calculation indicates that the uptake of the St monomer into NR particles is very rapid and the applied 3 h swelling time is generally sufficient to achieve a uniform distribution of the monomer within the seed latex particles. Figures 3 and 4 show conversion–time plots for the polymerization of 66.6 wt % St monomer based on NR in a not-crosslinked NR seed latex using different amounts of AIBN at various

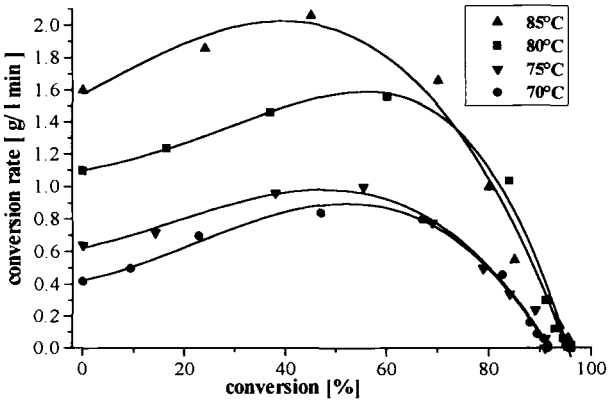

Figure 4 Conversion–rate plots for the polymerization of St in the presence of an NR seed latex using 0.40 wt % AIBN based on NR at 70, 75, 80, and 85°C. St/NR weight ratio: 40/60.

temperatures. A 1 L glass reactor was used for these preliminary trials. In Figure 3, the conversion–time plots for the polymerization of St in a not-crosslinked NR latex are plotted for different reaction temperatures.

Five hours were necessary to reach a conversion of more than 90% at 70 or 75°C. Increasing the temperature for 1.5 h from 70 to 85°C increased the degree of conversion to about 98%. Only 3 h were needed to polymerize 95% of the styrene monomer within the not-crosslinked NR latex particles when the monomer was polymerized at 85°C from the beginning. However, chain transfer to the NR macromolecules is enhanced by increase of the temperature since grafting reactions have a higher activation energy than that of the homopolymerization.[38–40] It is generally accepted that AIBN initiation does not promote grafting of St onto NR since AIBN cannot abstract hydrogen atoms from the NR backbone.[41,42] However, Soxhlet extraction and ^{1}H-NMR spectroscopy showed that NR chains had indeed been grafted at 75°C.[14] Degradation of NR chains has been reported in literature when St was polymerized in *cis*-1,4-polyisoprene using AIBN initiation.[43]

Figure 4 compares the polymerization rate-conversion plots for different reaction temperatures. The polymerization rate initially increased and rapidly fell off for conversions of more than 55%. Its shape can be interpreted as the result of the formation of PS microdomains within the NR phase. Due to the 0.2–2 μm size of the NR particles, small particle kinetics cannot be applied and it must be assumed that the polymerization is essentially a bulk-phase reaction. First, PS microdomains form and swell with the St monomer. PS subinclusions swell less with the St monomer than with the rubber phase. However, the polymerization rate is more rapid in the crosslinked PS domains than in the NR phase since the mobility of macroradicals is restricted in the thermoplastic phase. The viscosity within the microdomains is further increased by crosslinking of the PS subinclusions. As the polymerization proceeds, transport of the monomer takes place because the chemical potential of the monomer in the new phase domain is lower than in the rubber phase. Until conversions of 55%, the subinclusions grew and the rapid fall-off in polymerization rate can be explained by monomer depletion of the system.

To avoid grafting and degradation of the NR seed latex particles, a low polymerization temperature has to be chosen. At 60°C, an extremely long reaction time resulted (16 h) and 70°C was chosen for the further synthesis. Figure 5 compares the conversion–time plots for different initiator amounts at that temperature.

Using less AIBN mainly decreased the degree of conversion. The overall reaction time was not changed. AIBN, 0.40 wt %, based on NR was used in all further emulsion polymerizations in a 5 L stainless-steel reactor. Nearly 100% conversion could be achieved when the reaction temperature was increased to 85°C for 1.5 h after polymerizing more than 90% of the monomer at 70°C during 5 h. AIBN, 0.30 wt %, based on NR allowed us to attain only 95% conversion. The temperature profile used assured the lowest possible degree of grafting at an overall reaction time of 6.5 h. Low modulus, ungrafted NR particles are especially important since they are used as impact modifiers for thermoplastics.[28]

Influence of the St/NR Weight Ratio on the Particle Morphology

The morphology of 40% crosslinked PS/60% NR latex semi-IPN particles, which were synthesised by AIBN initiation in a 5 L stainless-steel reactor at 70°C, is shown in Figure 6. The TEM photomicrograph of these particles which have been incorporated into a PS matrix shows clearly that the styrene monomer polymerized in microdomains within the NR seed latex. Most of the secondary polymer resides in 150–250 nm-sized domains. Very small subinclusions (<50 nm) can also be seen. Large and small-sized spherical PS domains are distributed homogeneously throughout the NR phase.

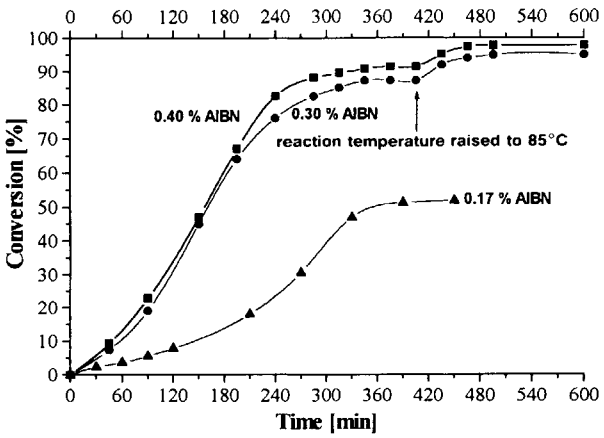

Figure 5 Conversion–time plots for the polymerization of St in the presence of a NR seed latex using 0.17, 0.30, and 0.40 wt % AIBN based on NR at 70°C. St/NR weight ratio: 40/60.

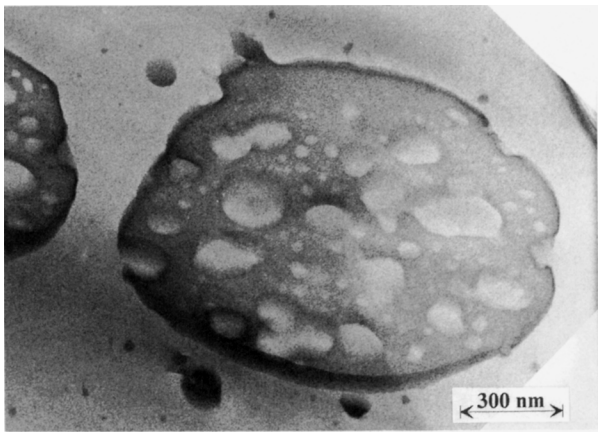

Figure 6 Transmission electron micrograph of an osmium tetroxide-stained ultramicrotome cut of a not-crosslinked NR-based particle containing 40 wt % crosslinked PS subinclusions. AIBN initiation at 70°C.

The morphology of 20% crosslinked PS/80% not-crosslinked NR latex semi-IPN particles which were synthesized by the same emulsion polymerization procedure is shown in Figure 7. Decreasing the styrene/NR weight ratio from 40/60 to 20/80 diminished the size of the PS subinclusions within the NR phase. Occlusions, 50–130 nm sized, were formed. Less St monomer decreased the mobility of the polymer chains due to an increase of the internal viscosity in the seed latex particles. Large-sized subinclusions with a more favorable free energy could not be formed. Figure 6 indicates that polymerizing 67 wt % St monomer based on the NR seed latex (St/NR weight ratio: 40/60) increased the mobility of the polymer chains within the latex particles and the case of a thermodynamic-controlled morphology with large-sized subinclusions is approached. Figure 8 shows that an inverted core (PS)–shell (NR) morphology could not be achieved by further raising the St/NR weight ratio to 60/40. This can be due to a slight degree of crosslinking of pure NR particles. It has to be mentioned that the presented particles also contain 25 wt % crosslinked PMMA which was polymerized in a second step by *tert*-BuHP/TEPA initiation to constitute a shell. The formation of the crosslinked PMMA shell around an occluded NR core, which is discussed in the following section, can be more clearly distinguished in Figure 16.

PS subinclusions, 200–400 nm sized, are visible. Their size increased considerably more than could be predicted. A maximal size of 250 nm is expected, assuming unchanged polymerization conditions. The very large PS subinclusions indicate that the viscosity within the NR particles which were swollen with 150 wt % St based on NR was very low. The inverse effect explains the formation of three to four times smaller-sized PS subinclusions in the case of NR particles containing only 20 wt % PS. However, the total number of subinclusions did not change when the styrene/NR ratio was varied.

Semicontinuous Emulsion Polymerization: Core–Shell Particle Synthesis

Core–particles were prepared by semicontinuous emulsion polymerization. The slow monomer feeding rate assured that newly nucleated particles are not formed or otherwise can be collected up during the preparation of the core–shell particles. The high solids content (50%) provided a large total surface area which facilitated the gathering of small particles which might have been newly nucleated. Colloidal stability of the latexes was assured by a very effective commercial nonylphenylether sulfate surfactant. The peroxide/amine-initiated emulsion polymerization yields very stable latexes since this initiation system introduces no additional ions into the NR latex and the ionic strength of the aqueous phase can be kept low. Figure 9 is a typical scanning electron photomicrograph of prevulcanized NR-based particles containing 40 wt % crosslinked PMMA in the shell. A core–shell arrangement of the polymer phases was assumed since the bipolar redox initiation system *tert*-BuHP/TEPA in conjunction with

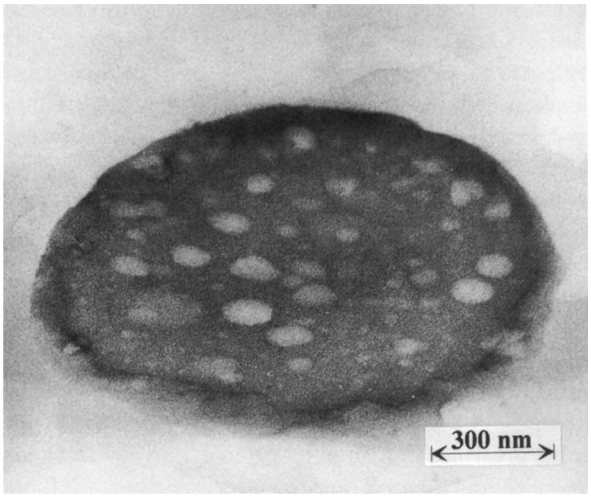

Figure 7 Transmission electron micrograph of an osmium tetroxide-stained ultramicrotome cut of a not-crosslinked NR-based particle containing 20 wt % crosslinked PS subinclusions. AIBN initiation at 70°C.

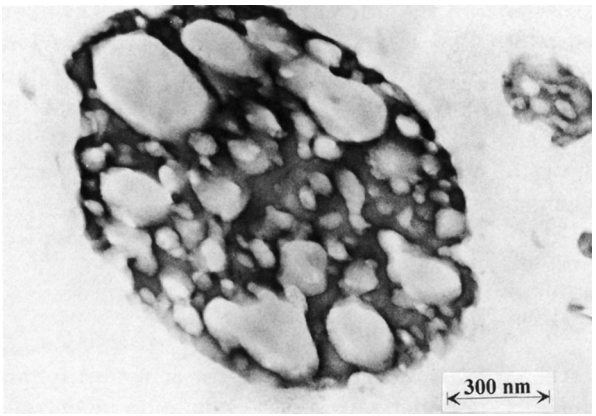

Figure 8 Transmission electron micrograph of an osmium tetroxide-stained ultramicrotome cut of a not-crosslinked NR-based latex particle containing 45 wt % crosslinked PS subinclusions within the rubber phase and 25 wt % crosslinked PMMA in the shell region. NR/PS ratio 40/60; subinclusion synthesis: AIBN initiation at 70°C; shell synthesis: *tert*-BuHP/TEPA initiation.

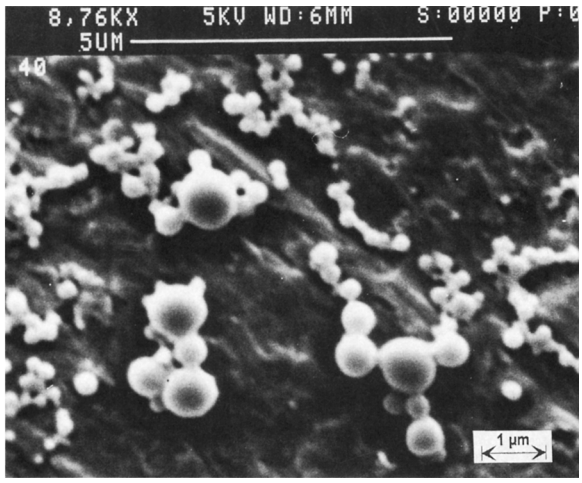

Figure 9 Scanning electron photomicrograph of prevulcanized NR-based latex particles containing 40 wt % crosslinked PMMA. *tert*-BuHP/TEPA initiation.

a semicontinuous feeding process was used. Free radicals are produced at the particle/water or monomer droplet/water interface since the peroxide is soluble in both the monomer and the NR particle, whereas the activator tetraethylene pentamine is water-soluble. It is reasonable to assume that the distribution of the secondary polymer (II) within the rubber particle is nonuniform with a polymer II-rich phase at the surface.

Polydisperse and isolated particles are clearly visible. Crosslinked PMMA, 40 wt %, in the particles was sufficient to form a closed shell around the vulcanized NR core to prevent the NR, with a glass transition temperature of −60°C, from film-forming. Scanning electron microscopy is well suited to demonstrate the extreme polydispersity of the NR-based particles. By light scattering, 580 nm was determined as the *z*-average mean size of the core–shell particles. Polymerizing 40 wt % crosslinked MMA in the 500 nm-sized NR seed latex should have increased its particle size to approximately 590 nm, which coincides with the measured particle size within experimental error. The polydisperse particle-size distribution curve of a precrosslinked NR latex containing 40 wt % crosslinked PMMA in the shell is plotted in Figure 10 as obtained by photon correlation spectroscopy performed on a Malvern Autosizer II.

Figure 10 shows that the plotted particle-size distribution curve corresponds to the actually observed particle sizes in Figure 9. Only very small (<250) particles, which are also present in NR latexes, could not be detected since very polydisperse latexes are difficult to measure exactly. In fact, photon correlation spectroscopy is best suited to determine a characteristic particle size and is considerably less sensitive to particle-size distribution.[44] The transmission electron photomicrographs in Figures 11 and 12 show that most of these small particles were NR-based core–shell particles and generation of a secondary crop of small pure PMMA particles could largely be avoided. The PMMA phase can be revealed by staining methods. For example, phosphotungstic acid (PTA) has been used to contrast PS/PMMA core–shell latexes.[45] This method was applied to prevulcanized NR particles containing 40 wt % PMMA.

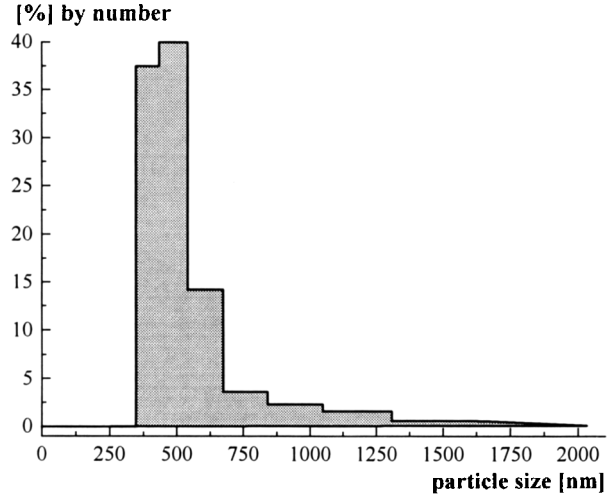

Figure 10 Particle-size distribution curve of a prevulcanized NR-based latex containing 40 wt % crosslinked PMMA. *tert*-BuHP/TEPA initiation.

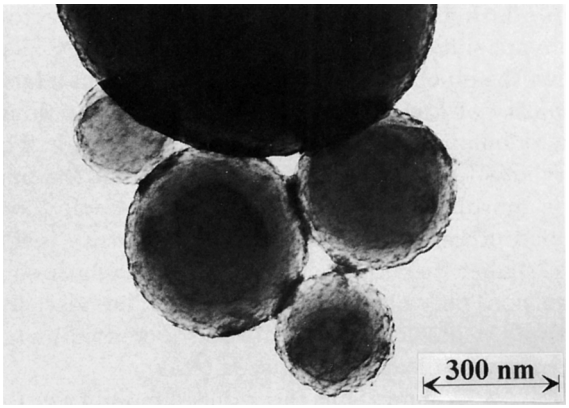

Figure 11 Transmission electron micrograph of phosphotungstic acid-stained prevulcanized NR-based latex particles containing 40 wt % crosslinked PMMA. *tert*-BuHP/TEPA initiation.

Figure 11 clearly shows the PMMA shell which has been stained by PTA. The lighter areas represent the PMMA phase. Of course, only the external region of the shell is formed by pure crosslinked PMMA which penetrated into the NR core. A latex IPN of crosslinked NR and crosslinked PMMA had been formed. The preparation technique did not allow us to observe the interior of the latex particles. To examine the morphology of the 60% prevulcanized NR/40% crosslinked PMMA latex IPN particles more closely, ultramicrotome cuts were studied by TEM. The particles were incorporated into a PS matrix for microtoming.

Figure 12 shows the actually obtained morphology of precrosslinked NR-based particles containing 40 wt % crosslinked PMMA. A perfect core–shell particle could not be achieved. Many very small 10–60 nm-sized PMMA subinclusions and a highly intermeshed PMMA shell/NR core interface region can be distinguished. The secondary polymer could not be restrained in a pure PMMA shell but meandered into the NR core. The obtained morphology of PMMA-coated NR particles is especially clear in the case of the small-sized particle in the upper-left corner of Figure 12. In fact, small-sized PMMA-grafted NR particles contain relatively more secondary polymer, since the thickness of the intermeshed PMMA/NR surface region does not vary appreciably with particle size. Centrifugal fractionation of *Heveaplus*-type NR particles led to the same conclusion.[23]

Both OsO_4 and PTA staining techniques show similar morphologies. Core–shell particles containing small-sized PMMA subinclusions were formed when the bipolar redox system *tert*-BuHP/TEPA

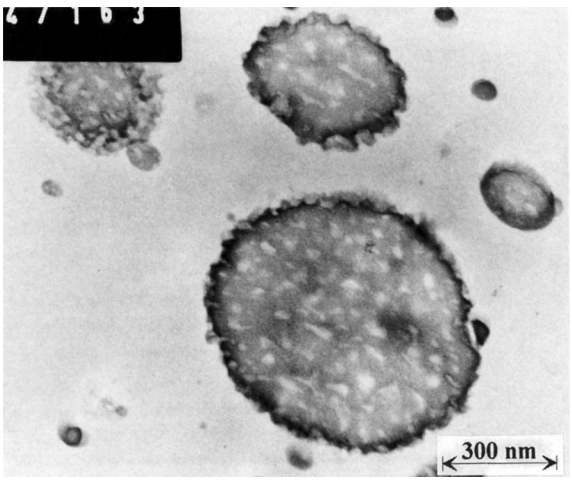

Figure 12 Transmission electron micrograph of an osmium tetroxide-stained ultramicrotome cut of prevulcanized NR-based particles containing 40 wt % crosslinked PMMA. *tert*-BuHP/TEPA initiation.

was used to polymerize MMA semicontinuously within a prevulcanized NR latex at 50°C. A similar morphology resulted for not-crosslinked NR-based latex particles containing 40 wt % crosslinked PMMA.

However, Figure 13 shows that the interface mixing is more extensive in the case of not-crosslinked rubber. It can be seen that the PMMA phase meandered from the exterior region into the center of the latex particle. Both composites, of not-crosslinked NR and prevulcanized NR-based particles, were

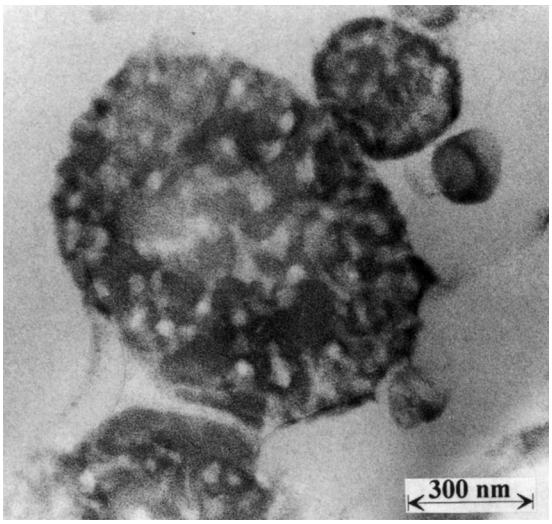

Figure 13 Transmission electron micrograph of an osmium tetroxide-stained ultramicrotome cut of not-crosslinked NR-based particles containing 40 wt % crosslinked PMMA. *tert*-BuHP/TEPA initiation.

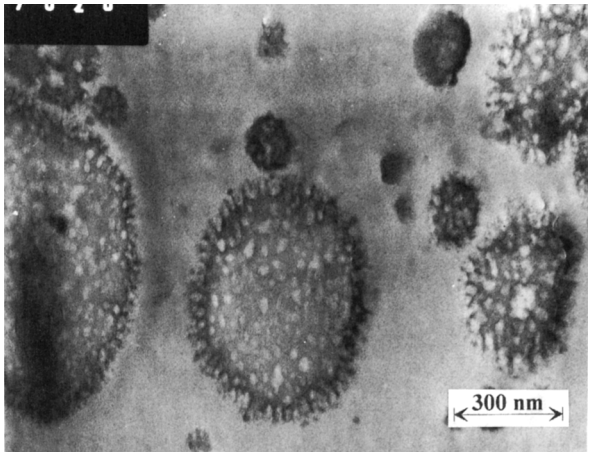

Figure 14 Transmission electron micrograph of the osmium tetroxide-stained ultramicrotome cut of not-crosslinked NR-based latex particles containing 40 wt % crosslinked PS in the shell. *tert*-BuHP/TEPA initiation.

prepared by the same emulsion polymerization process and the bipolar redox initiation system was used. Comparing Figures 12 and 13 shows that an increased crosslink density in polymer network I (prevulcanized NR seed latex) diminished the domain size of polymer II in the latex IPN. The tighter initial network restricted the size of the regions in which the secondary polymer PMMA could phase-separate. It is known that the crosslink density of polymer network I primarily controls the obtained IPN morphology.[46]

We also tried to create a very unpolar crosslinked PS shell around prevulcanized and not-crosslinked NR particles. Figure 14 indicates that a PS shell was much more difficult to obtain when the bipolar redox system and a semicontinuous procedure were used. Most of the monomer polymerized in very small microdomains within the NR core. The diffuse interface of the PS-grafted NR particle and the PS matrix indicates an external PS-rich layer. Pure NR or NR particles containing PS subinclusions (Figs. 6 and 7) have a distinctive phase boundary.

Thermodynamic considerations[5,47] applied to composite latex particles indicate that a polar PMMA shell around the hydrophobic NR core can be realized more easily. It is the minimizing of the interfacial tension of each phase which controls primarily the arrangement of the polymer phases in latex particles. The morphology with the lowest free-energy G will be taken up, i.e., the hydrophilic PMMA is concentrated in the shell region. The low reaction temperature (50°C) and the semicontinuous feeding process which ensured a small monomer concentration in the system reduced the chain mobility during the shell synthesis. These two factors were not sufficient to realize a very unpolar PS shell when the bipolar redox system was used, but a large quantity of the St monomer polymerized in small microdomains (5–30 nm) within the NR core. The very small PS subinclusions indicate that the particle morphology resulted from a kinetically controlled process caused by the high viscosity inside the rubber particles during the semicontinuous emulsion polymerization at 50°C. The viscosity within the particles can be further increased by the use of a prevulcanized NR seed latex.

Figure 15 shows that the reduced mobility of the polymer chains during semicontinuous polymerization of the St monomer within the precrosslinked NR latex particles decreased the PS subinclusion size by a factor 2. A further direct comparison of Figure 14 (semicontinuous feeding of the monomers) and Figure 6 (batch process), which are not-crosslinked NR-based particles containing 40 wt % crosslinked PS, illustrates how the viscosity within the latex particles controlled the particle morphology. The low viscosity in the monomer-swollen seed latex particles during the batch synthesis resulted in six times larger-sized subinclusions and the morphology was more thermodynamically controlled.

The 40% crosslinked PS/60% NR latex semi-IPN particles in Figure 6, which were synthesized by AIBN initiation during a batch emulsion polymerization, were subsequently coated with crosslinked PMMA using the bipolar redox initiation system *tert*-BuHP/TEPA and a semicontinuous feeding process. Figure 16 shows the morphology of these NR/crosslinked PS latex semi-IPN particles which were embedded in a PS matrix for microtoming.

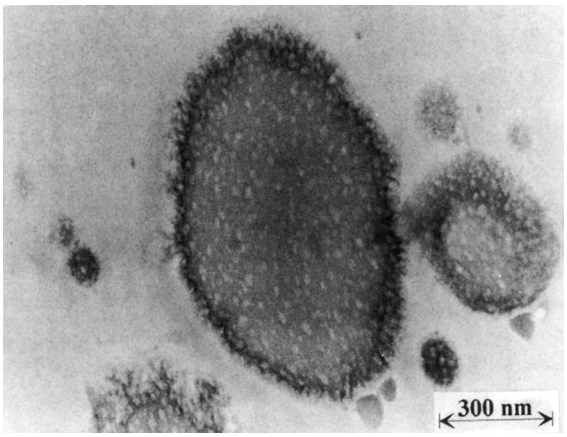

Figure 15 Transmission electron micrograph of the osmium tetroxide-stained ultramicrotome cut of a prevulcanized NR-based latex particle containing 40 wt % crosslinked PS in the shell. *tert*-BuHP/TEPA initiation.

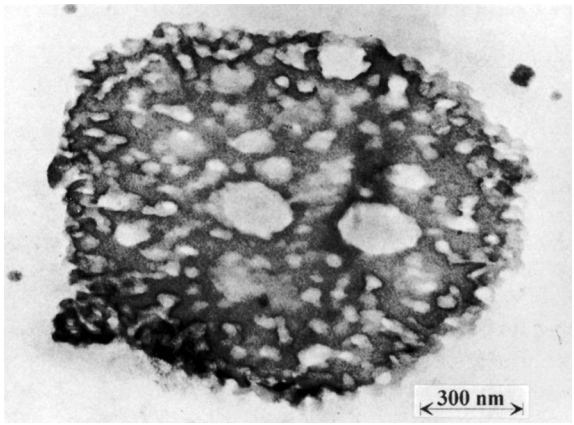

Figure 16 Transmission electron micrograph of the osmium tetroxide-stained ultramicrotome cut of a not-crosslinked NR-based latex particle containing 30 wt % crosslinked PS within the NR core and 25 wt % crosslinked PMMA in the shell. Subinclusion synthesis: AIBN initiation at 70°C; shell synthesis: *tert*-BuHP/TEPA initiation.

As in the case of ordinary PMMA-coated NR particles, it was not possible to avoid some of the PMMA (33 wt % based on the core polymer) also polymerizing within the nucleus of the semi-IPN seed latex particles. A 100–300 nm large intermeshed interface region between the crosslinked PS/NR latex semi-IPN core and the PS matrix can be clearly distinguished. It has to be noted though that the latex semi-IPN particles contained only half of the PMMA in comparison with the core–shell particle which is presented in Figure 13. Increasing the amount of the MMA monomer to 66 wt % based on the core semi-IPN resulted in the formation of more PMMA microdomains. Comparing PMMA coated not-crosslinked NR and crosslinked PS/NR semi-IPN based latex particles indicates that a crosslinked PMMA shell was easier to realize in the case of NR seed latex particles already containing 40 wt % crosslinked PS subinclusions. The PS subinclusions constrain the NR particles which swell less than do pure rubber particles and, consequently, the polymerization was more restricted to the surface region of the occluded NR particles. Figure 16 indicates that the PMMA phase meandered only about 100–300 nm into the semi-IPN core. The center of the particle was not reached as in the case of a non-crosslinked NR-based particle which is shown in Figure 13. Crosslinking of the PS subinclusions further impeded penetration of the MMA monomer to the center of the semi-IPN particles. A schematic representation of the latex IPN particles is proposed in Figure 23. It is assumed that the PS microdomains were interconnected by PS chains.

Effect of the Reaction Temperature on the Particle Morphology

The viscosity within the NR particles during the subinclusion synthesis is not only determined by the relative amount of the monomer which swells the rubber phase, but also the reaction temperature is another important factor to be considered. Figure 17 shows the morphology of NR based core–shell particles containing 40 wt % crosslinked PS subinclusions within the rubber phase which were synthesized at 85°C.

Increasing the reaction temperature from 70 to 85°C, which allowed us to decrease the reaction time for the subinclusion synthesis from 5 h to less than 3 h, resulted in larger-sized subinclusions due to a decrease of the internal viscosity during the preparation of the composite NR-based particles. Figure 17 shows that the subinclusion size increased from 150–200 nm to 200–400 nm. On the other hand, decreasing the reaction temperature to 60°C had only a little effect on the particle morphology: The subinclusions size decreased only marginally. The reaction temperatures of 70 and 60°C were both far below the glass transition temperature of PS (90°C).[48] The equation $T_g = T_{g\infty} - K/M_n$, where

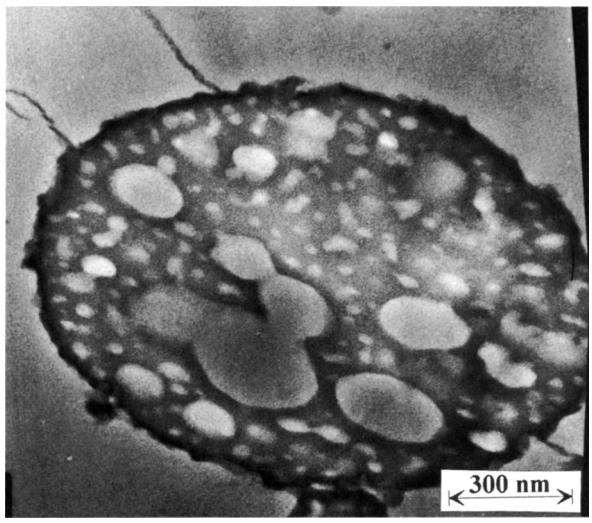

Figure 17 Transmission electron micrograph of the osmium tetroxide-stained ultramicrotome cut of a not-crosslinked NR-based latex particle containing 30 wt % crosslinked PS within the NR core and 25 wt % crosslinked PMMA in the shell. Subinclusion synthesis: AIBN initiation at 85°C; shell synthesis: *tert*-BuHP/TEPA initiation.

Table II Glass Transition Temperatures (T_g) of Different Composites of Not-crosslinked NR-based Latex Particles

NRR Particles Containing	Initiation System	T_g (°C)
40% PS subinclusions	AIBN	98
40% PS subinclusions	*tert*-BuHP/DMA	98
40% PS (core–shell particle)	*tert*-BuHP/TEPA	94
20% PS subinclusions	AIBN	97
20% PS subinclusions	*tert*-BuHP/DMA	97
20% PMMA (core–shell particle)	*tert*-BuHP/TEPA	104
40% PMMA (core–shell particle)	*tert*-BuHP/TEPA	106
25% PMMA in the shell and 30% PS in the core	*tert*-BuHP/TEPA AIBN	104 96

$T_{g\infty}$ = 100°C and $K = 1.0 \times 10^5$,[49] predicts that the mobility of growing PS chains with a number-average molecular weight M_n of more than 3300 (70°C reaction temperature) or 2500 (60°C) is very restricted at the reaction temperatures used which were below their respective glass transition temperatures. At 85°C, growing PS chains are mobile up to an M_n of 6700, which allows the secondary polymer to phase separate in larger-sized subinclusions. The St monomer present plasticized PS and NR, facilitating further the phase separation.

NR particles containing crosslinked PS subinclusions can also be prepared at 50°C using the hydrophobic redox initiation system *tert*-BuHP/DMA. The resulting subinclusions size was not considerably decreased either, in comparison to particles prepared by AIBN initiation at 70°C.

Differential Scanning Calorimetry

Differential scanning calorimetry (DSC) can be used for the evaluation of the miscibility between components of polymer blends.[50] In the absence of miscibility, a composite of two polymers exhibits two distinct glass transitions of the pure components. The glass transition temperature (T_g) of the noncrosslinked NR latex was −63°C. Two comprehensive studies concerning the glass transition temperature of NR reported −71°C (Ref. 51) and −67°C (Ref. 52) as the true T_g. These differences are due to different sample preparation, pretreatment, and the correction methods used. However, our main objective was to measure the glass transition temperature of the secondary polymers within the NR particles. Clear identification of the glass transition of the PS or PMMA phase in NR-grafted copolymers is difficult to realize experimentally.[53,54] The composition and the glass transition temperatures of different composite NR-based latex particles are given in Table II.

Two glass transition temperatures were observed for all modified NR latexes, consistent with a two-phase morphology, as confirmed by TEM. The lower glass transition temperature of the NR phase (−63°C) was not influenced by the composition of the latex particles. The upper glass transition temperature of the PMMA and PS phase could be observed without prior annealing. It was possible to observe separately the PS and the PMMA transitions in NR-based latex particles containing 30 wt % crosslinked PS in subinclusions and 25 wt % crosslinked PMMA in the shell. Increasing the amount of the secondary polymers in the latex particles improved the resolution of the DSC measurements. The determined values of the glass transition temperatures of PMMA (104°C) and PS (97°C) closely coincide with pure PMMA and PS. The literature reported 104°C for the T_g of PMMA[55] and 90°C for the T_g of PS.[48] The measured high T_g for the PS phase can be explained by a relatively high molecular weight of the PS chains. The limiting glass transition temperature for PS is 100°C at very high molecular weights.[56]

Dynamic Mechanical Analysis

Dynamic mechanical analysis (DMA) is a technique often used to characterize phase behavior in polymer blends.[57] In Figure 18, the experimental data of the loss tangent, tan δ, are plotted as a function of the temperature for a cast film of pure NR particles and for a film of NR particles containing 40 wt % crosslinked PS subinclusions which were synthesized by AIBN initiation at 70°C. The composite particle morphology is shown in Figure 6.

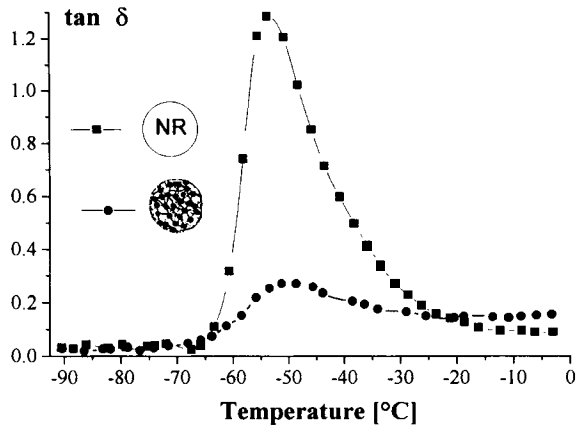

Figure 18 Comparison of tan δ of cast films of a pure NR latex and NR particles containing 40 wt % crosslinked PS subinclusions synthesized by AIBN initiation at 70°C.

Each curve in Figure 18 shows a peak indicating the dynamic transition of the not-crosslinked NR phase. The polymers are well phase-separated since the width of the tan δ peaks of pure NR and NR containing PS subinclusions did not change. In the case of NR particles containing crosslinked PS subinclusions, the amplitude $(\tan \delta)_{max}$ decreased considerably and the location of the dynamic transition temperature T_d shifted from −54°C (pure NR) to −51°C. It is known that the dynamic transition of a composite material is directly related to the relative amount of the measured component.[58,59] However, the observed large decrease of the amplitude $(\tan \delta)_{max}$ must be interpreted not only as a consequence of a reduction of the present rubber phase which has been substituted by the PS subinclusions but also it appears that the relative rubber quantity "active" in the dynamic transition is reduced. This reduction is due to a partial immobilization of the rubber chains by grafting of PS. The increase of T_d can also be explained by rubber grafting. DSC did not allow us to detect grafting of the NR phase. As may be expected, the glass transition temperature of NR is lower than the dynamic transition temperature.

Thermogravimetric Analysis

NR rubber-based composite latex particles have been incorporated into thermoplastics to increase their impact resistance.[27-29,60] They must be stable at processing temperatures of 200 or 270°C for about 3–5 min depending on the toughened polymer matrix. The molten thermoplastic, which contains the NR-based particles, usually is well protected from contact with atmospheric oxygen. Assuming the worst possible case, dried NR particles were exposed to a flow of ordinary air and heated at a constant rate of 10°C/min until 800°C to analyze their degradation behavior at elevated temperatures.

Figure 19 shows that a crosslinked PMMA shell protects the NR phase from degradation. The temperature for the maximum rate of decomposition (T_{max}) could be shifted from 365°C for pure NR to 380°C in the case of core–shell particles. Of course, (T_{max}) depends on the heating rate, e.g., a faster heating rate of 30°C/min increases (T_{max}) to 412°C.[61] The prepared PS-coated NR particles were not studied since PMMA protects the NR more effectively against oxidation. In fact, the oxygen permeability of PS is 25 times higher than is the permeability of PMMA.[62] The difference of the thermal stabilities of PMMA and NR are not big enough to observe two separated peaks. Alternative methods for measuring the thermal performance of modified NR particles are DSC and Fourier transformation infrared spectroscopy.[63,64] The oxidation products which are formed during the degradation of NR at elevated temperatures are described in the literature.[65]

Film Formation

The film-forming ability of composite latexes can be interpreted in terms of the morphology of the particles achieved. Poor film formation (cracked film) is a sign of a high concentration of the secondary polymer at the surface of the particles and good film formation (coherent film) characterizes composite NR particles with an even distribution of polymer II within the NR seed latex particles.[22] Two mm-thick films of the different NR-based core–shell particles were prepared by evaporating the water of

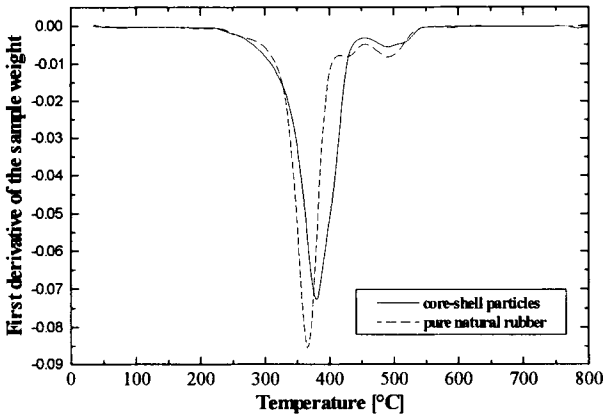

Figure 19 Comparison of the degradation behavior of pure NR and NR-based core–shell particles containing 40 wt % crosslinked PMMA. *tert*-BuHP/TEPA initiation.

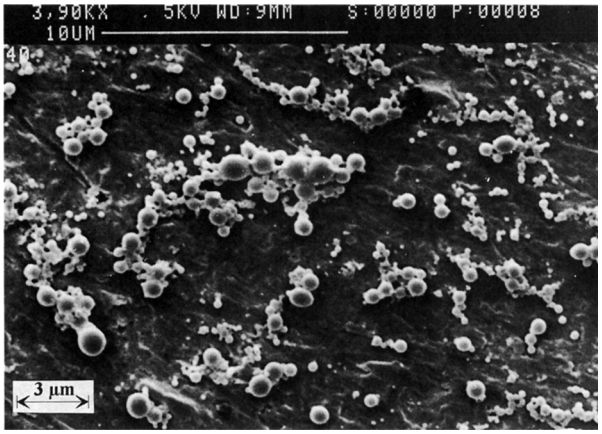

Figure 20 SEM photo of not-crosslinked NR-based latex particles containing 40 wt % crosslinked PMMA in the shell. *tert*-BuHP/TEPA initiation.

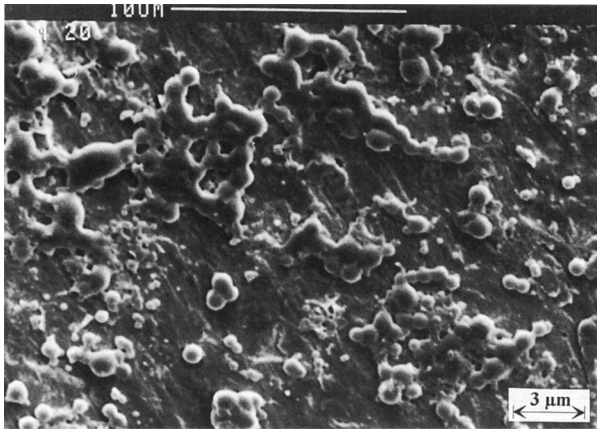

Figure 21 SEM photo of not-crosslinked NR-based latex particles containing 20 wt % crosslinked PMMA in the shell. *tert*-BuHP/TEPA initiation.

different NR latexes during 1 week at 23°C and 50% relative humidity. Information already in the literature[22] describes cracks observed in the case of NR-based latex particles containing more than 20 wt % crosslinked PMMA in the shell. The SEM photo of Figure 9 shows that 40 wt % crosslinked PMMA in the shell of prevulcanized NR-based latex particles prevented the NR phase from forming a film. Polymerizing the same mass fraction of crosslinked PMMA in a not-crosslinked NR seed latex also yielded hard and isolated particles as shown in Figure 20. Both latexes were prepared by a semicontinuous feeding process in combination with the bipolar redox initiation system *tert*-BuHP/TEPA. Free radicals are generated at the particle/water interface and the secondary polar polymer PMMA is concentrated in the exterior region of the composite latex particle.

Figure 21 shows that decreasing the amount of crosslinked PMMA in the shell of not-crosslinked NR-based latex particles to 20 wt % PMMA still allowed us to observe many isolated particles. However, the latex begins to recover film integrity.

Figure 20, and especially Figure 21, show that neighboring NR-based core–shell particles without PS subinclusions have a tendency to coalesce. Core–shell particles containing PS subinclusions within the NR phase were also studied. Figure 22 shows an SEM photo of 60% NR/40% PS latex semi-IPN-based particles containing 25 wt % PMMA in the shell. The increased magnification allows us to discern clearly that occluded NR-based core–shell particles which are touching each other maintained their integrity.

Hard and isolated latex particles can be seen. This result is in accordance with the actually observed morphology of the latex particles in Figure 16. PMMA could be more effectively concentrated in the shell region of the latex IPN-based particles which did not form a film.

The obtained films of not-crosslinked NR latex particles containing 40 wt % crosslinked PS in the shell were clearly more homogeneous than in the case of PMMA-coated particles. These qualitative observations signify that the ideal core–shell structure is easier to achieve in the case of a PMMA than for a PS shell. This is consistent with the TEM observations and thermodynamic considerations.

When initiation by the fully oil-soluble redox system peroxide/DMA or by AIBN was used, the emulsion polymerization took place entirely within

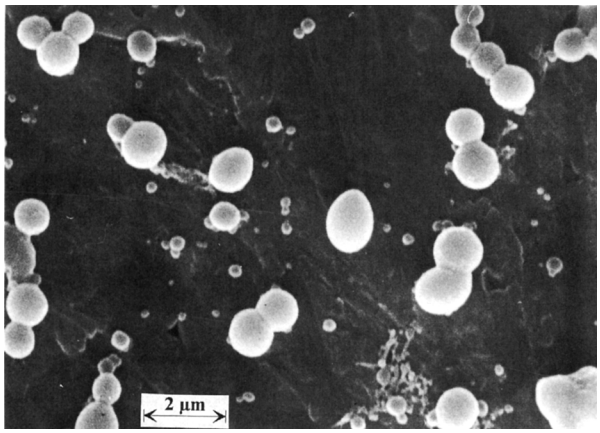

Figure 22 SEM photo of not-crosslinked NR-based latex particles containing 30 wt % crosslinked PS within the NR core and 25 wt % crosslinked PMMA in the shell. Subinclusion synthesis: AIBN initiation at 70°C; shell synthesis: *tert*-BuHP/TEPA initiation.

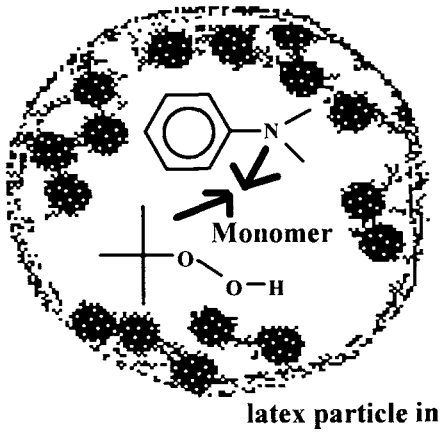

Figure 23 Site of the reaction in a composite NR-based latex particle in the case of AIBN initiation or the hydrophobic redox initiation system *tert*-BuHP/DMA. Batch process.

the NR particles and a rather uniform distribution of the secondary polymer in PS subinclusions within the latex particles was observed by TEM. Hence, not-crosslinked NR particles containing 20 or 40 wt % PS subinclusions, synthesized by these initiation systems, formed a homogeneous film. This means that the NR phase formed the soft matrix in which PS subinclusions were embedded. The morphology of the prepared film must be very similar to the not-crosslinked NR particles containing 20 or 40 wt % PS subinclusions which are shown in Figures 6 and 7. Lastly, it is known that γ-radiation-induced copolymerization produces radicals which are generated in both the aqueous and the organic phase and an intermediate distribution of polymer II within the NR particles results.[20]

POLYMERIZATION SITE AND MECHANISM OF MORPHOLOGY FORMATION

On the basis of these TEM photos, a mechanism for the development of the different composite NR-based latex particles is proposed. The emulsion polymerization feeding processes and the different initiation systems used determined the morphology of the observed latex particles.

When an inverted structure is required, the secondary polymer usually is produced by batch polymerization in the presence of a seed latex.[66] The initiation system used for the introduction of PS subinclusion into not-crosslinked NR particles is schematically represented in Figure 23. The initiator AIBN or the redox couple *tert*-BuHP/DMA are soluble in the organic phase and the polymerization takes place entirely within the NR particle.

Before the polymerization was initiated by increasing the temperature to 70°C, the NR particles were uniformly swollen by the St monomer. As soon as the polymerization starts, by the generation of free radicals, phase separation occurs and PS domains form throughout the NR seed latex particles. The existing PS microdomains grow and new domains form. The polymerization kinetics which are presented in Figure 4 are in accordance with this picture. Higher St/NR swelling ratios decreased the viscosity within the rubber particles and the increased diffusion rate of radicals and polymer chains resulted in the formation of larger-sized subinclusions. Photon correlation spectroscopy, TEM, and SEM show that NR latexes contain particles with a wide range of diameters from 0.1–2 μm. Most of the particles are less than 0.5 μm, but most of the mass of the rubber resides in particles greater than 0.6 μm. It is assumed that the polymerization within the NR seed latex particles is essentially a bulk polymerization.

A bipolar redox initiation system in conjunction with a semicontinuous feeding process produces NR-based core–shell particles. The location of the components of the redox couple *tert*-BuHP/TEPA is shown in Figure 24.

The semicontinuous feeding process maintained a low monomer concentration absorbed at or near the surface of the NR seed latex particles where the redox partners meet and the emulsion polymerization takes place. A low reaction temperature (50°C) and crosslinking raised the kinetic barrier to phase inversion. The crosslinking agent, introduced during the polymerization of MMA or St, helped to concentrate the secondary polymers at the particle surface since the polymer phases were locked into a

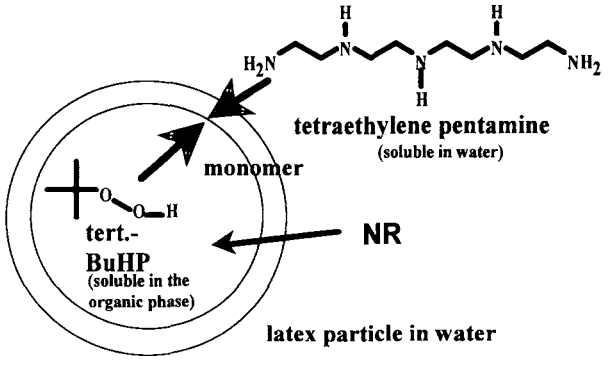

Figure 24 Site of the reaction in a composite NR-based latex particle in the case of the bipolar redox initiation system *tert*-BuHP/TEPA. Semicontinuous process.

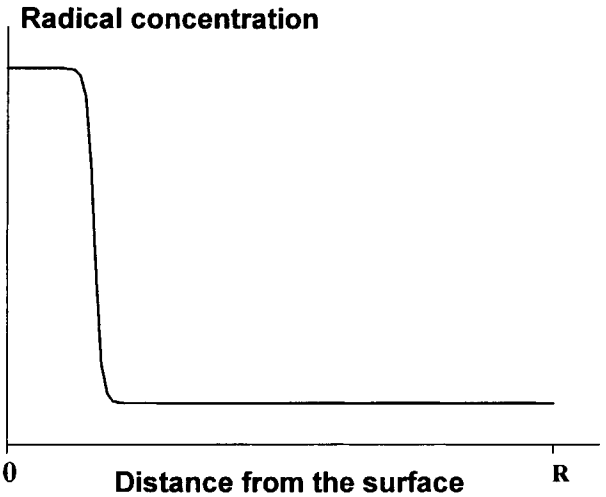

Figure 25 Schematic representation of the radical distribution profile within the latex particles when the bipolar redox initiation system *tert*-BuHP/TEPA is used in conjunction with a semicontinuous feeding process.

core–shell configuration.[67] Grafting of the secondary polymers onto NR chains is promoted by the peroxide initiation system used. This fact increases the stability of the core–shell arrangement of the polymer phases by reducing the mobility of the polymer chains.[68] It was easier to concentrate polar PMMA in the shell region of the latex particles than was PS which formed many very small-sized subinclusions within the rubber phase. Comparing NR particles containing the same amount of PS, which were synthesized either by a batch (hydrophobic redox system) or a semicontinuous (bipolar redox system) process, decreased the size of the internal PS domains by a factor 6. This change reflects a transition from a more thermodynamically controlled morphology to a more kinetically controlled one. A low monomer concentration, in the case of the semicontinuous process, did not allow the PS phase to form large-sized domains because of a high viscosity within the rubber particles. An inverted core–shell particle would be the arrangement with the lowest free-energy G.

The polymerization rate in a bulk polymerization decreases rapidly at high conversions since the propagation rate coefficient k_p is reduced. A recent publication explains this effect by a decreased initiator efficiency.[69] At high conversions, the possibility of the recombination of radicals is increased since the higher viscosity within the latex particles reduces the diffusion rate of the generated radicals. The monomer concentration in the latex particles was very low since the semicontinuous feeding process assured starved feeding conditions; e.g., at the end of the monomer addition period, more than 90% of the fed monomer had already been polymerized. Radicals which are generated in the surface region of the particles cannot diffuse quickly due to the high viscosity within the NR particles. At the surface, the radical concentration is considerably higher than in the center of the latex particle since this is the site of their generation. Furthermore, radical pairs can be separated by a desorption of one radical into the aqueous phase which contributes to increase the initiation efficiency there. A radical distribution curve is proposed in Figure 25. The positions R and O on the x-axis represent the center of a latex particle and the particle/water interface, respectively. Due to the complexity of the bipolar redox initiation, a quantitative approach to this problem was not tried.

CONCLUSIONS

PMMA- and PS-grafted NR latex particles were prepared. Both vulcanized and not-crosslinked natural rubber seed latexes were used. Several initiation systems allowed us to control the site of polymerization which determined the final morphology of the prepared composite NR-based particles. The mode of monomer addition was also highly influential in determining the particle morphology. TEM in combination with different staining methods made it possible to observe the morphology of the prepared latexes actually obtained. It was possible to adjust the emulsion polymerization process of NR latexes in such a way that the resulting latexes of identical chemical composition possessed either a heterogeneous structure, with the secondary polymer concentrated in the shell region of the particles, or a more homogeneous structure, with polymer II evenly distributed in small-sized subinclusions within the NR particles.

AIBN initiation or the hydrophobic redox initiation system *tert*-BuHP/DMA served for the introduction of rigid PS subinclusions within the NR particles during batch emulsion polymerization. A higher monomer/NR swelling ratio produced larger-sized crosslinked PS subinclusions within the NR phase. A reaction temperature which approached the glass transition temperature of PS allowed the secondary polymer to phase-separate in large-sized PS subinclusions.

A semicontinuous emulsion polymerization process, in conjunction with the bipolar redox initiator couple *tert*-BuHP/TEPA, served for the preparation of NR-based core–shell particles at 50°C. This type

of initiation favors the particle/water interface as the locus of polymerization. Polar PMMA was much more likely to produce the desired core–shell morphology than was PS. A perfect crosslinked PMMA shell could not be obtained but the secondary polymer meandered into the NR-based core. The use of prevulcanized NR diminished the core/shell interface mixing and decreased the PS subinclusion size. NR particles containing PS subinclusions restrained the PMMA phase to the surface region of the composite NR particles. A semicontinuous feeding process decreased the PS subinclusions size by a factor of 6 in comparison with a batch reaction. SEM clearly shows hard particles in the case of more than 20% crosslinked PMMA in the shell of NR particles. NR-based core–shell particles containing PS subinclusions were clearly less susceptible to coalescence. Differential scanning and DMA confirmed a two- or three-phase particle morphology.

The authors would like to take this opportunity to thank the European Economic Community for financing this research project (BRITE-EURAM Project BE-4260). The assistance of Mr. Morvan of the Centre de Géochimie de la Surface in Strasbourg for the transmission electron studies is also gratefully acknowledged.

REFERENCES

1. W. J. LeFevre and K. G. Harding, U.S. Pat. 2,460,300 (1949).
2. E. B. Bradford and J. W. Vanderhoff, *J. Polym. Sci.*, **C3,** 41 (1960).
3. J. M. Gloaguen, P. Heim, P. Gaillard, and J. M. Lefebvre, *Polymer,* **33,** 4741 (1992).
4. J. C. Daniel, *Makromol. Chem. Suppl.,* **10/11,** 359 (1985).
5. Y.-C. Chen, V. Dimonie, and M. El-Aasser, *J. Appl. Polym. Sci.,* **42,** 1049 (1991).
6. M. Okubo, A. Yamada, and T. Matsumoto, *J. Polym. Sci. Polym. Chem. Ed.,* **16,** 3219 (1980).
7. S. Shen, M. S. El-Aasser, V. L. Dimonie, J. W. Vanderhoff, and E. D. Sudol, *J. Polym. Sci. A,* **29,** 857 (1991).
8. I. Cho and K. W. Lee, *J. Appl. Polym. Sci.,* **30,** 1903 (1985).
9. V. L. Dimonie, M. S. El-Aasser, and J. W. Vanderhoff, *Polym. Mater. Sci. Eng.,* **58,** 821 (1988).
10. G. F. Bloomfield, *Rubb. Dev.,* **5,** 34 (1952).
11. G. F. Bloomfield and P. McL. Swift, *J. Appl. Chem.,* **5,** 609 (1955).
12. D. J. Hourston and J. Romanie, *Eur. Polym. J.,* **25**(7/8), 695 (1989).
13. D. J. Hourston and J. Romanie, *J. Appl. Polym. Sci.,* **39,** 1587 (1990).
14. D. J. Hourston and J. Romanie, *J. Appl. Polym. Sci.,* **43,** 2207 (1991).
15. R. N. Mathurajah, *Malaysian Rubb. Planter's Bull.,* **74,** 131 (1964).
16. Natural Rubber Producers Research Association, Technical Information Sheet No. 9, Revised 1977.
17. B. C. Sekhar, *Rubber Chem. Technol.,* **31,** 430 (1958).
18. E. H. Andrews and D. T. Turner, *J. Appl. Polym. Sci.,* **3**(9), 366 (1960).
19. E. Cockbain, T. D. Pendle, and D. T. Turner, *Chem. Ind. (Lond.)* 759 (1958).
20. E. Cockbain, T. D. Pendle, and D. T. Turner, *J. Polym. Sci.,* **39,** 419 (1959).
21. P. W. Allen, G. Aurey, C. G. Moore, and J. Scanlan, *J. Polym. Sci.,* **36,** 55 (1959).
22. R. J. Ceresa, *Block and Graft Copolymerization,* Wiley-Interscience, London, 1973, Vol. 1, p. 47.
23. P. W. Allen, *Chemistry and Physics of Rubberlike Substances,* L. Bateman, Ed., MacLaren, London, 1963, p. 97.
24. E. H. Andrews and D. T. Turner, *J. Appl. Polym. Sci.,* **3**(9), 366 (1960).
25. P. W. Allen, C. L. M. Bell, and E. G. Cockbain, *Rubb. Chem. Technol.,* **33,** 825 (1960).
26. L. H. Sperling, *Interpenetrating Polymer Networks and Related Materials,* Plenum Press, New York, 1981.
27. M. Schneider, T. Pith, and M. Lambla, *Polym. Adv. Technol.,* **6,** 326 (1995).
28. M. Schneider, T. Pith, and M. Lambla, to appear.
29. M. Schneider, T. Pith, and M. Lambla, in PAT 95, *Third International Symposium on Polymer for Advanced Technology,* June 11–15, 1995, Pisa, Italy, p. 90.
30. K. Kato, *J. Electron Microsc.,* **14,** 220 (1965).
31. K. Kato, *Polym. Lett.,* **4,** 35 (1966).
32. M. Matsuo, C. Nozaki, and Y. Jyo, *Polym. Eng. Sci.,* **9,** 197 (1969).
33. C. S. Baker and D. Barnard, *Polym. Prepr.,* **26,** 29 (1985).
34. H. Hasma and A. Subramaniam, *J. Nat. Rubb. Res.,* **1**(3), 30 (1986).
35. P. W. Allen, C. L. M. Bell, and E. G. Cockbain, in *Proceedings of the International Rubber Conference (Washington),* 1959, p. 521.
36. A. R. Behrens and H. B. Hopfenberg, *J. Membr. Sci.,* **10,** 283 (1982).
37. J. Crank and G. S. Park, Eds., *Diffusion in Polymers,* Academic Press, London, 1968.
38. R. A. Hayes, *J. Polym. Sci.,* **11,** 531 (1953).
39. G. Smets and M. Claesen, *J. Polym. Sci.,* **8,** 289 (1952).
40. R. A. Gregg and F. R. Mayo, *J. Am. Chem. Soc.,* **75,** 3530 (1953).
41. A. Brydon, G. M. Burnett, and G. G. Cameron, *J. Polym. Sci.,* **2,** 3255 (1973).
42. G. G. Cameron and M. Y. Qureshi, *J. Polym. Sci.,* **18,** 2143 (1980).
43. V. V. Pchelintsev, L. M. Ivanova, K. B. Piotroviskii, and T. V. Dikina, *Zh. Prikl. Khim.,* **51,** 2367 (1978).

44. R. L. Rowell and J. R. Ford, *Emulsion Polymers and Emulsion Polymerization,* D. R. Bassett and A. E. Hamielec, Eds., ACS Symposium Series 165, American Chemical Society, Washington, DC, 1981, p. 85.
45. Y.-C. Chen, V. Dimonie, and M. S. El-Aasser, *Macromolecules,* **24,** 3779 (1991).
46. A. A. Donatelli, L. H. Sperling, and D. A. Thomas, *J. Appl. Polym. Sci.,* **21,** 1189 (1977).
47. D. Sundberg, A. Casassa, J. Pantazopoulos, and M. Muscato, *J. Appl. Polym. Sci.,* **41,** 1425 (1990).
48. F. P. Reding, J. A. Fancher, and R. D. Whitman, *J. Polym. Sci.,* **57,** 483 (1962).
49. T. G. Fox and P. J. Flory, *J. Polym. Sci.,* **14,** 315 (1954).
50. O. Olabisi, L. M. Robeson, and M. T. Shaw, *Polymer–Polymer Miscibility,* Academic Press, New York, 1979, Chap. 3.
51. C. Kow, M. Morton, L. J. Fetters, and N. Hadjichristidis, *Rubb. Chem. Technol.,* **55,** 245 (1982).
52. D. R. Burfield and K. L. Lim, *Macromolecules,* **16,** 1170 (1983).
53. P. M. Toporowski and J. E. L. Roovers, *J. Polym. Sci. Polym. Chem. Ed.,* **14,** 2233 (1976).
54. G. Krause and M. Iskander, *Multiphase Polymers,* Advances in Chemistry Series, 176, S. L. Cooper and G. M. Estes Eds., American Chemical Society, Washington, DC, 1979, p. 205.
55. J. C. Wittmann and A. J. Kovacs, *J. Polym. Sci. C,* **16,** 4443 (1969).
56. T. G. Fox and P. J. Flory, *J. Appl. Phys.,* **21,** 581 (1950).
57. D. R. Paul and S. Newman, Eds., *Polymer Blends,* Academic Press, New York, 1978, Vol. 1, Chap. 5.
58. N. G. McCrum, *J. Polym. Sci.,* **27,** 555 (1958).
59. K. H. Illers and E. Jenckel, *Kolloid-Z. Z. Polym.,* **160,** 97 (1958).
60. M. Schneider, T. Pith, and M. Lambla, *Eight Major International Conference Within Polymat '94,* Imperial College, London, UK, Sept. 19–22, 1994, p. 571.
61. W. C. Wake, M. J. R. Loadman, and B. K. Tidd, *Analysis of Rubber and Rubber-like Polymers,* 3rd ed., Applied Science, London, 1983, p. 138.
62. Kirk-Othmer, *Encyclopedia of Chemical Technology,* Wiley, New York, 1978, Vol. 3, p. 481.
63. R. Arnaud and R. de Monte, *Caoutchouc Plast.,* **708,** 95 (1991).
64. D. W. Brazier, *Rubb. Chem. Tech.,* **53**(3), 437 (1980).
65. M. Farmer, *Rubb. Chem. Tech.,* **62**(2), G47 (1989).
66. G. A. Vandezande and A. Rudin, *J. Coat. Technol.,* **66**(828), 99 (1994).
67. S. Lee and A. Rudin, in ACS Symposium Series 492, E. S. Daniels, E. D. Sudo, and M. S. El-Aasser, Eds., American Chemical Society, Washington, DC, 1992, p. 234.
68. T. I. Min, A. Klein, M. S. El-Aasser, and J. W. Vanderhoff, *J. Polym. Sci. Polym. Chem. Ed.,* **21,** 2845 (1983).
69. G. T. Russel, D. H. Napper, and R. G. Gilbert, *Macromolecules,* **21,** 2141 (1988).

Received September 21, 1995
Accepted February 1, 1996